



Long-term carbon storage in Brazilian Cerrado soils – a conjunction of wildfires, bioturbation, and local edaphic controls on vegetation

Judith Schellekens · Marina Justi · Rodrigo Macedo ·
Márcia Regina Calegari · Peter Buurman · Thomas W. Kuyper ·
Plínio Barbosa de Camargo · Pablo Vidal-Torrado

Received: 13 June 2022 / Accepted: 28 November 2022 / Published online: 7 December 2022
© The Author(s), under exclusive licence to Springer Nature Switzerland AG 2022

Abstract

Purpose The objective of this study is to improve our understanding of soil organic matter (SOM) stability in Brazilian Cerrado, by interpreting soil properties at the ecosystem scale and elaborating on the interactions of biotic, climatic and edaphic controls.

Methods Three 2 m soil profiles with significantly different total organic carbon TOC content but located on the same geomorphological unit were studied for $\delta^{13}\text{C}$ isotopic composition to connect tree-grass patterns to TOC content. To gain insight into soil carbon stability, C/N, $\delta^{13}\text{C}$ and $\delta^{15}\text{N}$ were analysed for functional organic matter (OM) pools: free particulate OM (POM), occluded POM, base-extractable OM, and mineral-associated OM.

Results Small but abrupt shifts of $\delta^{13}\text{C}$ with depth reflected simultaneous changes in tree-grass vegetation patterns over the past 10,000 years in all three profiles. These temporal changes were superimposed on spatial differences as indicated by consistent differences in $\delta^{13}\text{C}$ values between the profiles, reflecting that site-specific differences in tree-grass patterns persisted over the past 10,000 years. Profiles with a historically larger contribution from trees (as evidenced by lower $\delta^{13}\text{C}$) had increased charcoal contents. Downward movement of charcoal by intense

Responsible Editor: Hans Lambers.

Highlights

- Variation in soil C storage at the ecosystem scale was studied for Cerrado Ferralsols.
- Abrupt shifts in $\delta^{13}\text{C}$ depth records reflected tree abundance during the Holocene.
- Local edaphic factors had higher impact on tree abundance than climatic changes.
- Soils with high C content had historically more trees, more BC, and faster bioturbation.

Supplementary Information The online version contains supplementary material available at <https://doi.org/10.1007/s11104-022-05824-4>.

J. Schellekens (✉) · M. Justi · R. Macedo ·
P. Vidal-Torrado
Soil Science Department, Luiz de Queiroz Agriculture
College, University of São Paulo, Av. Pádua Dias 11,
Piracicaba, São Paulo CEP 123418-900, Brazil
e-mail: schellekens.j@hetnet.nl

M. R. Calegari
College of Geography, Western Paraná State
University - UNIOESTE, Campus Marechal Cândido
Rondon, Rua Pernambuco, 1777, P.O. Box 91,
Marechal Cândido Rondon, Parana State CEP 85970-000,
Brazil

R. Macedo
National Institute of Semi-Arid, Av. Francisco Lopes
de Almeida, S/N, P.O. Box 10067, Campina Grande,
Paraíba CEP 58429-970, Brazil

P. Buurman
Water Systems and Global Change Group, Wageningen
University, P.O. Box 47, 6700 AA Wageningen,
The Netherlands

bioturbation occurred faster in the OM-rich soils as suggested by ^{14}C dating.

Conclusion We found that long-term carbon storage in Brazilian Cerrado soils was a conjunction of wildfires, bioturbation, and local edaphic controls on tree-grass composition. Soils with an OM-rich thick A-horizon had more trees, more charcoal, and a higher activity of soil macrofauna, which was related to local differences in soil water availability.

Keywords Cerrado ecosystems · Bioturbation · Black carbon · $\delta^{13}\text{C}$ and $\delta^{15}\text{N}$ isotopic composition · Umbric Ferralsols

Introduction

Savannahs play a significant role in the global carbon cycle with their large below-ground carbon storage, seasonal burning, and vegetation dynamics (Scurlock and Hall 1998). On a global scale, edaphic and climatic factors are controls on soil carbon stocks (Luo et al. 2021). At the ecosystem scale, climatic factors are the same, but in dryland ecosystems a high degree of local variability in soil carbon pools was found (Smith and Waring 2019). Understanding variation in soil carbon storage at the ecosystem scale may contribute to improve modelling of soil-climate feedback mechanisms. The Brazilian Cerrado represents the largest area of savannah in the Neotropics (Bueno et al. 2018), and harbours soils with a thick A-horizon rich in OM next to soils without such large carbon content. These soils, classified as Umbric Ferralsols (IUSS Work Group WRB 2015), cover 258,839 km² of the world, of which the major part is on old surfaces in southern Brazil (Marques et al. 2015; Silva and Vidal-Torrado 1999). Apart from their abundant occurrence in the (sub)tropics, Ferralsols are particularly relevant in soil carbon storage due to their strongly weathered deep profiles, causing a relatively uniform distribution of carbon to great depth (Klamt and Van Reeuwijk 2000; Martinez et al. 2021).

The large contrast in soil carbon content at short distance within the Cerrado suggests important controls on soil carbon stability that act at a very local scale. The stability of soil carbon is frequently studied from different perspectives but mostly focussing on a single component (e.g., mineral-association, aggregate protection, microbial vs plant material), resulting in a lack of studies with a more holistic approach (Angst et al. 2021). This lack of integrating disciplines is even reinforced in the Cerrado, with the dynamic forest-grass vegetation patterns and wildfires that are both extremely sensitive to changes in climatic conditions. The objective of this study is to contribute to our understanding of soil carbon storage in Umbric Ferralsols of the Cerrado, by examining all of the biotic, climatic and edaphic controls at the ecosystem scale. Furthermore we aim at elaborating on the potential interactions of vegetation patterns, soil properties, soil biota and environmental factors in relation to soil carbon stability in this ecosystem.

Information on vegetation patterns is stored in Cerrado soils by the intense and ongoing activity of soil fauna with time (Schaefer 2001). Therefore, past environmental changes can be preserved in these soils and used to study the effects of vegetation on soil carbon (Chiapini et al. 2018; Pessenda 1996, Pessenda et al. 1998). To examine the factors that control soil carbon content, we studied the vertical variation in soil properties and soil organic matter (SOM) composition for three 2 m soil profiles from a preserved natural Brazilian Cerrado fragment. The selected soil profiles are located in the same geomorphological unit and have a clear difference in SOM content. Bulk soil samples were studied for $\delta^{13}\text{C}$ isotopic composition and compared with ^{14}C dating to reconstruct temporal changes in tree-grass vegetation patterns (Calegari et al. 2013; Dümig et al. 2008; Pessenda et al. 2004), and connect these to total organic carbon (TOC) content.

To gain insight in soil carbon stability several SOM fractions were isolated, including free particulate organic matter (POM), occluded POM (i.e., enclosed in aggregates), base-extractable OM, and mineral-associated OM. These SOM fractions represent different functional pools in terms of soil carbon persistence (e.g., Angst et al. 2021; Justi et al. 2017). The free POM is considered less stable fraction, while the occluded POM is protected in aggregates. The base-extractable OM represents more decomposed OM, which predominantly reflects OM

T. W. Kuyper
Soil Biology Group, Wageningen University, P.O. Box 47,
6700 AA Wageningen, The Netherlands

P. Barbosa de Camargo
Centre of Isotopic Energy in Agriculture, University
of São Paulo, Piracicaba, Brazil

that is weakly bound to soil minerals. The mineral-associated fraction is considered most stable because it is strongly bound to soil minerals and/or consists of hydrophobic OM (von Lützow et al. 2006). The SOM fractions were studied for $\delta^{13}\text{C}$ and $\delta^{15}\text{N}$ isotopic composition and C/N, which together provide information on SOM sources and its decomposition (Prietz et al. 2020; Six et al. 1998; Wiesmeier et al. 2019). Furthermore, the composition of SOM was compared with clay content, charcoal content (>2 mm), and bioturbation (micromorphology). This approach allows to examine biotic, climatic and edaphic controls on soil carbon storage at the ecosystem scale in the Cerrado.

Materials and methods

Location

The area of Grão Mogol represents natural Brazilian Cerrado biome (Nepstad et al. 1997) that is classified as Cerrado sensu stricto (IBGE 2012; Fig. 1). A list of species is given in Table S1. It is located on the northern plateau of the Serra do Espinhaço (Minas Gerais state, Brazil; Fig. S2). Three Umbric Ferralsols (IUSS Work Group WRB 2015) were sampled in this area. Two profiles had a thick (>100 cm) dark-coloured A-horizon and are classified as Panto Umbric Ferralsol (Profundihumic), profiles P1-H (16°16'16" S; 42°58'50" W) and P2-H (16°18'01" S; 43°03'22" W), and will be referred to as Ferralsol with deep humic

horizon. At a distance of 0.5 km from profile P2-H we sampled the third profile with a thinner Umbric horizon, classified as Xanthic Umbric Ferralsol, i.e., without both Panto characteristics and Profundihumic qualifier (profile P3-L; 16°17'18" S; 43°03'04" W). Thus, the acronyms of the profiles refer to the TOC content, which is relatively high (P1-H and P2-H) or low (P3-L). The study area is located on a Neogenic geomorphic surface (850 m a.s.l.). The three profiles had the same topographic position on a flat summit (Fig. S2) and were described and sampled to a depth of 2 m.

Soil sampling

Samples of 0.1 kg were obtained at 10 cm depth intervals (except for the interval between 150 and 200 cm for profile P2-H, for which samples were exclusively taken according to pedogenic horizon as described below). The air-dried and sieved (2 mm) soil samples were used to determine the content and isotopic composition of carbon.

A second sample set with samples of 1 kg was obtained for all pedogenetic horizons, resulting in 7 to 9 samples per profile, making 24 samples in total. The SOM fractionation was performed on these samples, and these SOM fractions were analysed for elemental and isotopic composition of both carbon and nitrogen.

The samples obtained from pedogenic horizons were previously studied by Justi et al. (2017) to understand the long-term degradation effects on black

Fig. 1 Representative image of the actual vegetation in the study area. A list of plant species in the area is given in Table S1



carbon (BC) in these soils. Analysis included physicochemical properties and the quantity of macroscopic charcoal (>2 mm). The data are given in Table S3. Additionally, pyrolysis–gas chromatography–mass spectrometry (pyrolysis–GC/MS) was performed on the SOM fractions by Justi et al. (2017). The pyrolysis–GC/MS equipment parameters, methodology for data analysis, and a list of quantified pyrolysis products are given in Supplementary material S4-1. In the present study we use the pyrolysis data to support interpretations from elemental and isotopic analysis. Thin sections of most horizons were prepared by Justi et al. (2017) for micromorphological study of charcoal. These thin sections were revisited here to examine the bioturbation process. For detailed methodology of thin sections we refer to Justi et al. (2017).

¹⁴C dating

Charcoal layers were found in all three profiles. Radiocarbon dating was carried out by Beta Analytic Radiocarbon Laboratory (Miami, USA) using AMS on charcoal fragments (Justi et al. 2017) and humin. Humin was separated according to Pessenda (1996) and represents the SOM that remains after i) (ultrasonic) wet sieving over 0.200 mm to remove particulate organic matter, ii) repeated treatment with a 0.1 M pyrophosphate and sodium hydroxide solution to remove humic- and fulvic acids, and iii) acid hydrolysis with 3 M HCl at 100 °C to eliminate organic residues such as sugars and proteins. Radiocarbon age of charcoal layers was analysed on a homogenised mixture of about 10 charcoal fragments from the layer. Ages are expressed as calibrated years before present (cal. years BP) with accuracy of $\pm 2\sigma$. The calibration was performed according to the SHCal13 curve using the software CALIB Rev 7.0.4 (Reimer et al. 2013).

SOM fractionation

All 24 soil horizon samples were used for sequential fractionation of SOM. Particulate OM was separated by density before and after aggregate disruption, representing the free POM and the occluded POM, respectively. After removal of the POM fractions, weakly bound SOM was isolated with a classical alkaline extraction (0.1 M NaOH; 1/10 w/v), i.e.,

base-extractable OM. The soil residue that remained after NaOH extraction was demineralised with hydrofluoric acid and represents the mineral-associated OM. Detail on the SOM fractionation procedure and the fractionation scheme is given in Supplementary material S5. In the following we use “mineral soil fractions” to refer to the group of base-extractable OM, mineral-associated OM, and bulk soil samples.

Content and isotopic composition of carbon and nitrogen

All bulk samples sampled at 10 cm depth intervals were analysed for TOC content and $\delta^{13}\text{C}$. Soil OM fractions and bulk soil of the samples that were taken according to pedogenic horizon were analysed for TOC and N content, C/N ratio, and $\delta^{13}\text{C}$ and $\delta^{15}\text{N}$ isotopic composition. Analysis was performed at CENA/USP (Piracicaba, Brazil) via dry combustion with a CNHO elemental analyser coupled to a Carlo Erba® Delta Plus mass spectrometer. The isotope ratios are expressed in the δ -notation with an analytical precision of 0.1‰: $\delta^{13}\text{C}$ (‰) = $[\text{R}_{\text{sample}} / \text{R}_{\text{standard}} - 1] \times 1000$, where: R_{sample} and $\text{R}_{\text{standard}}$ refer to the $^{13}\text{C}/^{12}\text{C}$ ratios of the sample and the standard. Similarly, $\delta^{15}\text{N}$ (‰) = $[\text{R}_{\text{sample}} / \text{R}_{\text{standard}} - 1] \times 1000$, where: R_{sample} and $\text{R}_{\text{standard}}$ refer to the $^{14}\text{N}/^{15}\text{N}$ ratios of the sample and the standard.

The $\delta^{13}\text{C}$ depth records sampled at 10 cm depth interval were used to evaluate temporal changes and spatial differences in the relative contribution of C_3 and C_4 plants, as they differ in $\delta^{13}\text{C}$ (C_3 plants range from -32‰ to -22‰, while C_4 plants range from -17‰ to -9‰). In savannah ecosystems the woody component is exclusively of the C_3 photosynthetic pathway, while the C_4 component is mainly represented in grasses (Boutton et al. 1998). Therefore, $\delta^{13}\text{C}$ values of SOM can be used to assess tree-grass dynamics in the Cerrado. Variations in soil $\delta^{13}\text{C}$ can be influenced by other factors than vegetation changes (e.g., decomposition), therefore a limit of 4‰ is generally used to reflect vegetation changes (Desjardins et al. 1996). However, because the studied profiles are located in the same Cerrado ecosystem, shifts in $\delta^{13}\text{C}$ depth records that are lower than 4‰ will also be linked to past changes in vegetation composition when they are both abrupt and consistent for several consecutive samples.

Data analysis

Because the profiles are located within a distance of 10 km from each other it can be assumed that the response of the vegetation cover to climatic changes was into the same direction. Based on the direction of abrupt shifts in $\delta^{13}\text{C}$ (enrichment or depletion) and taking into account the age of the charcoal layers, depth intervals of the different profiles were assigned to a time period (Dümig et al. 2008). Within a profile, each selected depth interval thus represents a time period with similar vegetation cover (according to $\delta^{13}\text{C}$). We are aware that the samples within a given time period cannot be considered as repetitions because they were not independent. However, the means of $\delta^{13}\text{C}$ and TOC content of bulk samples were analysed for significant differences by ANOVA. This was done to provide statistical support for the selected time periods, and to compare the corresponding depth intervals within and between profiles.

The properties of bulk soil that was sampled per pedogenic horizon were statistically analysed by principal component analysis to visualise the main factors that influenced carbon storage (Supplementary material S6). Depth records are used to visualise minor but consistent differences between profiles, between SOM fractions, or with depth. If mentioned, relationships between variables are given as coefficient of determination (r^2) and were considered significant at $P < 0.05$.

Results

^{14}C dating of charcoal and humin

The results of ^{14}C dating of charcoal fragments and humin are given in Fig. 2 and Table S7. All three profiles contain charcoal fragments of different size in the soil matrix and two visible charcoal layers. Radiocarbon age of charcoal indicates maximum ages of at least 7897 ± 58 cal. years BP, 7620 ± 45 cal. years BP and 9603 ± 65 cal. years BP in profiles P1-H, P2-H and P3-L, respectively. Ages of both charcoal layers from profile P1-H correspond to those in profile P2-H (with a maximum difference of 290 years), while ages from those in profile P3-L are between 2182 and 1700 years older. Ages of charcoal increased with depth within each profile.

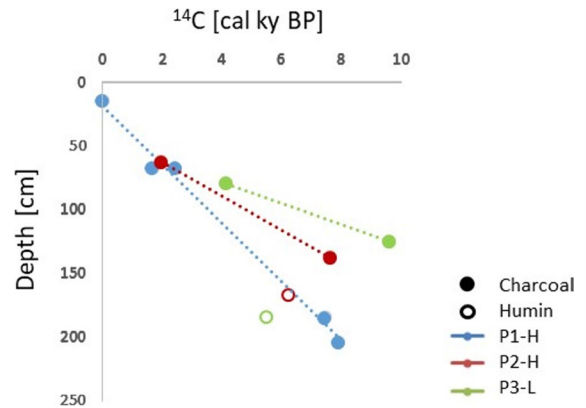


Fig. 2 ^{14}C ages of charcoal and humin plotted against depth. Note that open symbols reflect humin samples, while filled symbols reflect charcoal samples. The profiles are indicated by P1-H, P2-H and P3-L, in which H and L stand for relatively high or low TOC content

The increase of age with depth was strongest in the sequence P3-L > P2-H > P1-H, indicating that profile P1-H had relatively younger charcoal at similar depth than profile P3-L (Fig. 2). Humin ^{14}C values reflect mean residence times instead of absolute ages, which explains its relatively low ^{14}C values compared to charcoal (Fig. 2).

TOC and $\delta^{13}\text{C}$ of bulk soil sampled at 10 cm intervals

Records of $\delta^{13}\text{C}$ isotopes for bulk soil samples are given in Fig. 3. In the upper 30 cm, all three profiles showed a gradual decrease towards the surface of $\delta^{13}\text{C}$ (5‰ in profile P3-L, 3‰ in P1-H, and 2‰ in P2-H), which is probably due to recent environmental changes such as shrub encroachment, resulting in more negative $\delta^{13}\text{C}$. Below 30 cm, $\delta^{13}\text{C}$ varied between -23‰ and -18‰ and showed some abrupt shifts within each profile, with maximum differences of 2.3‰, 1.7‰ and 0.7‰ for profiles P3-L, P2-H, and P1-H, respectively; these shifts are marked by the dashed lines in Fig. 3. Accordingly, depth ranges that correspond to the same time periods in the three profiles are indicated by periods I–V in Fig. 3.

The ranges of time periods and corresponding depth intervals, and mean values of $\delta^{13}\text{C}$ and TOC content for each time period are provided in Table 1. Because the range of the decrease in the surface (5‰ to 2‰) is much larger than that of the shifts deeper in the profile (2.3‰ to 0.7‰),

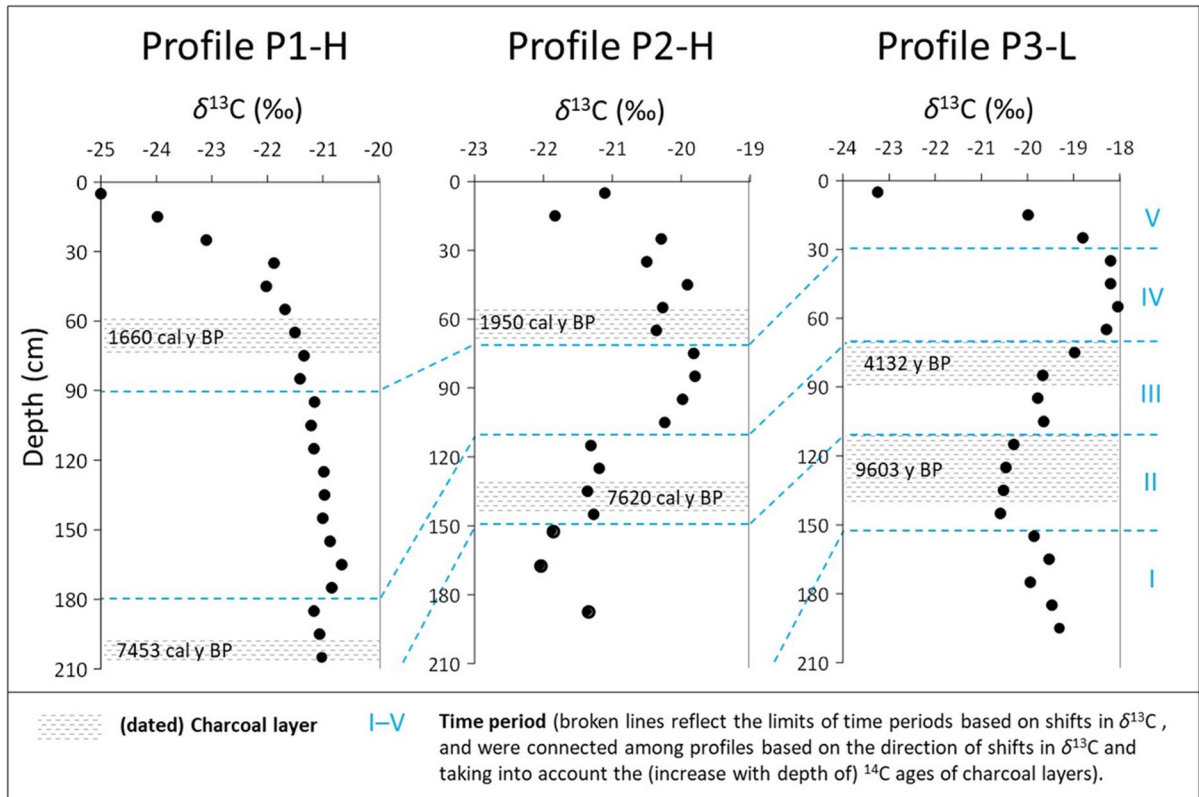


Fig. 3 Depth records of $\delta^{13}\text{C}$ isotopes for bulk soil samples. The profiles are indicated by P1-H, P2-H and P3-L, in which H and L stand for relatively high or low TOC content. Note that because of the relatively large increase in $\delta^{13}\text{C}$ from 0–30 cm, this depth interval is not taken into account by calculating averages that are presented in Table 1 (see "TOC and $\delta^{13}\text{C}$ of bulk soil sampled at 10 cm intervals" section). The lower

limit of period V in profile P3-L falls entirely within the upper 30 cm, while in the other profiles the lower limit of this period is at larger depth; thus for period V, mean values of $\delta^{13}\text{C}$ were not interpreted in profile P3-L, while calculation of the mean of this period in the other profiles started below the 30 cm limit. Furthermore, periods I and II were not present in all profiles within the depth of 2 m

the upper 30 cm will be excluded for comparison of the means of period V. Average $\delta^{13}\text{C}$ values significantly differed between profiles, with -21.2‰ , -20.5‰ , and -19.5‰ in profiles P1-H, P2-H, and P3-L, respectively. In addition, mean $\delta^{13}\text{C}$ values increased in the same profile sequence for equally aged layers (Table 1; periods I and V were not compared among profiles, because period I is not present in the sampled depth range of profiles P1-H and P2-H, while period V fully coincides with the upper 30 cm in profile P3-L). TOC content decreased with depth, and for equally aged layers it was systematically higher in the sequence

P1-H > P2-H > P3-L (Table 1, Fig. 4a). Irrespective of the gradual decrease of TOC with depth, the shifts observed in ^{13}C records were also identified for TOC content (Table 1).

Composition of SOM fractions

C/N, $\delta^{15}\text{N}$ and $\delta^{13}\text{C}$ records of SOM fractions and bulk soil samples for pedogenic horizons are given in Fig. 5. A positive correlation for $\delta^{15}\text{N}$ and $\delta^{13}\text{C}$ was found for bulk samples within each profile ($r^2=0.80$, 0.31 and 0.75 for profiles P1-H, P2-H and P3-L, respectively). Bulk samples of profile P3-L showed

Table 1 Ranges of charcoal ¹⁴C ages and corresponding depth intervals, and average TOC and δ¹³C values for bulk samples (sampled at 10 cm intervals) for each assigned time period for the three profiles (P1-H, P2-H, and P3-L)

Period	Depth (cm)			¹⁴ C age (cal. years BP)		Ave. δ ¹³ C (‰) ^a			Ave. TOC (%) ^a		
	P3-L	P2-H	P1-HI	Minimum	Maximum	P3-L	P2-H	P1-H	P3-L	P2-H	P1-H
V ^b	0–30	0–70	0–90	present	> 1950						
IV	30–70	70–110	90–180	> 1950	< 4132	-18.2 (0.10)	-20.3 (0.25)	-21.7 (0.27)	0.71 (0.07)	1.68 (0.13)	2.28 (0.28)
III	70–110	110–150	180–200+	< 4132	> 7897	-19.5 (0.36)	-21.3 (0.07)	-21.1 (0.07)	0.62 (0.05)	1.11 (0.19)	0.88 (0.08)
II	110–150	150–200+		< 7620	> 9603	-20.5 (0.12)	-21.7 ^c (0.36)		0.47 (0.03)	0.82 ^c (0.18)	
I	150–200+			> 9603		-19.6 (0.27)			0.33 (0.02)		
I-V	0–200	0–200	0–200			-19.5	-20.5	-21.2			

^a Standard deviation between brackets; Differences are significant for age intervals within each profile (columns) and between profiles within the same age interval (rows), for both δ¹³C (*P* < 0.0001 for the ANOVA test) and TOC (*P* < 0.004);

^b Upper 30 cm not considered;

^c Values according to the sample set that is sampled per horizon

significantly higher values of δ¹⁵N and δ¹³C, and significantly lower C/N values than both P-H profiles (Table 2). Within each profile there was no significant negative correlation between C/N and δ¹³C and between C/N and δ¹⁵N (*r*² < 0.15).

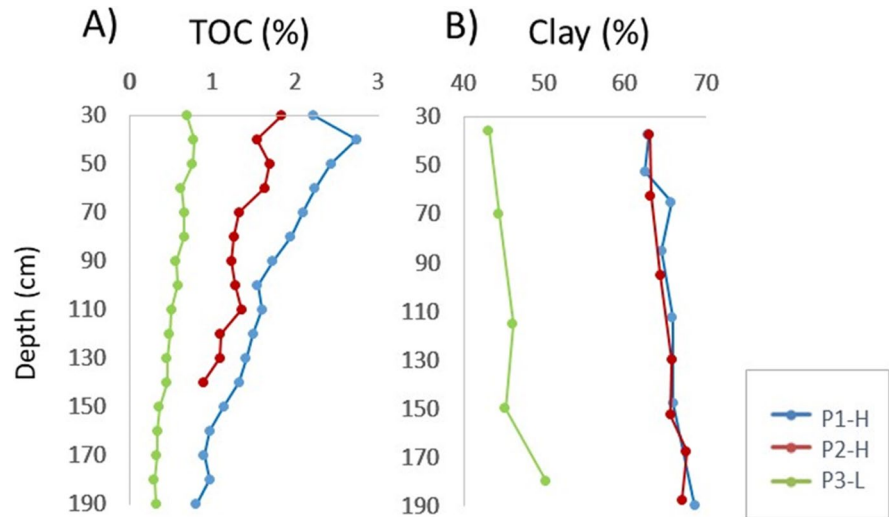
Values of C/N, δ¹³C and δ¹⁵N of the base-extractable and mineral-associated SOM fractions were similar to bulk soil, while the POM fractions clearly differed from those of the mineral soil fractions (Fig. 5). δ¹³C varied from -25.6‰ to -17.7‰ in the mineral soil fractions, while the POM fractions showed about 4‰ lower values over the whole depth range and varied from -27.9‰ to -23.9‰. Similarly to δ¹³C, δ¹⁵N also showed consequently lower values for POM fractions compared to mineral soil fractions; δ¹⁵N varied between -1.3‰ and 4.9‰ in the POM fractions (except for one occluded POM sample with 7.5‰), and between 3.9‰ and 9.8‰ in the mineral soil fractions. C/N and δ¹⁵N showed a negative correlation among all fractions (*r*² = 0.64, Fig. S8). For the base-extractable and mineral-associated SOM fractions, profile P3-L showed significantly lower C/N and higher δ¹³C and δ¹⁵N values compared to the P-H profiles (Table 2), and the POM fractions systematically showed lower values for C/N in profile P3-L for equally aged layers (Fig. 5).

The δ¹³C depth trend within each profile in the bulk samples was maintained in the POM fractions (0.28 < *r*² < 0.76). Contrary to δ¹³C, δ¹⁵N depth records of the POM fractions did not exhibit a significant positive correlation with those of bulk samples (except for the occluded POM in profiles P2-H and P3-L; Fig. 5).

The mean abundance of groups of pyrolysis products for each profile and fraction is given in Table S4-2. Compared to both P-H profiles, profile P3-L had a lower contribution from aromatics in all fractions except base-extractable OM, a lower contribution from aliphatic products in mineral-associated OM, and a larger contribution from carbohydrates in mineral-associated OM and POM fractions.

The degradation state of SOM was examined in the plant-derived component by the composition of lignin phenols in the mineral-associated OM fraction (Supplementary material S4-3, Fig. S4c). The mineral-associated OM fraction was chosen because the POM fractions (free and occluded POM) are not considered appropriate to judge SOM degradation state as it consists of relatively undecomposed litter and charcoal,

Fig. 4 Depth records of (a) TOC content of bulk soil samples (sampled at 10 cm intervals), and (b) clay content (sampled per horizon). The profiles are indicated by P1-H, P2-H and P3-L, in which H and L stand for relatively high or low TOC content



while the extremely low lignin content in the base-extractable fraction (<0.3%, Supplementary material S4-2, Table S4-2) makes this fraction less reliable to interpret the composition within the lignin group. Support was provided by indices of polyaromatic pyrolysis products that reflect the degradation state of BC (Supplementary material S4-3, Fig. S4ab).

Micromorphology

Thin sections demonstrate intense bioturbation in all profiles and at all depths (Fig. S9), by abundant i) rounded and oval microaggregates with well-developed microgranular structure in an enaulic relative distribution, and ii) features ascribed to faunal activity including biological channels with dominant loose and both continuous and discontinuous infillings. A visual comparison of these features showed no clear difference between profiles in the intensity of bioturbation.

Discussion

Differences in vegetation composition ($\delta^{13}\text{C}$ of bulk samples, and charcoal)

Temporal differences (climatic changes)

The presence of charcoal over the whole depth of all three profiles (Table S3) suggests frequent wildfires over the whole time period, while layers with

concentrated charcoal represent intense fire events. The increase in ^{14}C age of charcoal with depth (Fig. 2) reflects an ongoing input of charcoal with time (Marques et al. 2015; Pessenda et al. 2004; Silva and Vidal-Torrado 1999) because relatively coarse material, such as charcoal and stones, sinks downwards due to the active upward transport of fine particles by termites and other soil macrofauna (Schaefer 2001; Wilkinson et al. 2009).

$\delta^{13}\text{C}$ varied between -26‰ and -19‰ , in agreement with a mixed vegetation of C_3 (trees and shrubs) and C_4 (grasses) plants in natural Cerrado systems (Calegari et al. 2013; Jantalia et al. 2007; Pessenda et al. 1998; Roscoe et al. 2000; Table S1). Water availability is one of the main drivers that control tree density both between and within Cerrado ecosystems, with drier conditions limiting tree growth (Eiten 1972). Both spatial differences and temporal changes in tree-grass composition (as indicated by $\delta^{13}\text{C}$) thus likely reflect changes in water availability. Drier conditions are suggested by enrichment in $\delta^{13}\text{C}$ from periods II (before 8000 years BP) < III (from 8000–4000 years BP) < IV (from 4000–2000 years BP). These changes in vegetation cover were relatively minor ($\delta^{13}\text{C}$ ranging from -18.0‰ to -21.7‰ in periods II–IV) but in most cases abrupt, suggesting periods with stable tree-grass composition, i.e., strong fire-vegetation feedbacks (Oliveras and Malhi 2016). The $\delta^{13}\text{C}$ enrichment from period III to IV was clearly present in all profiles and indicates an increase of C_4 grasses, suggesting relatively drier conditions. Drier conditions during period IV are in good

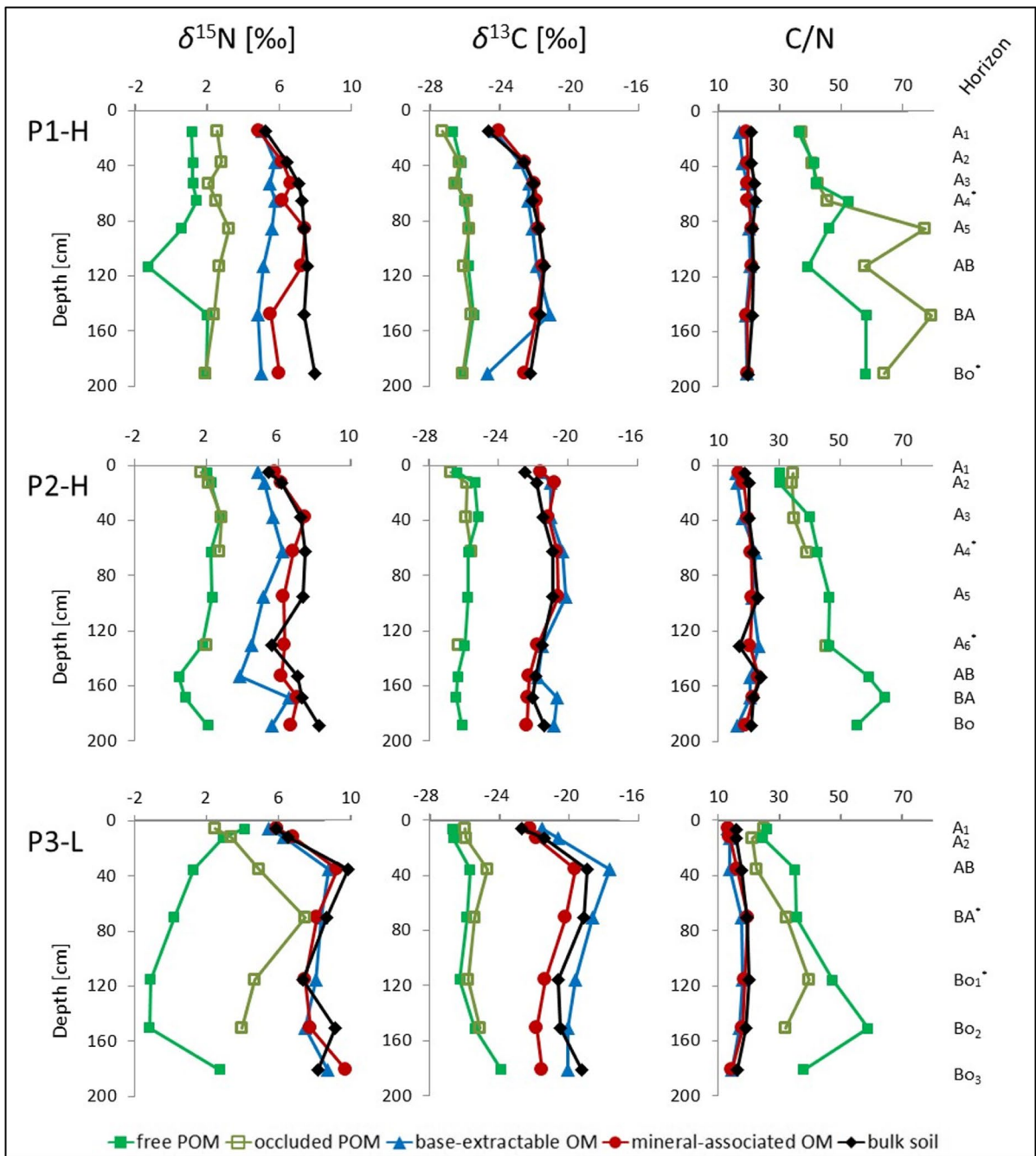


Fig. 5 Depth records of $\delta^{13}\text{C}$ and $\delta^{15}\text{N}$ isotopes and C/N for bulk samples and SOM fractions in the three profiles. The profiles are indicated by P1-H, P2-H and P3-L, in which H and L

stand for relatively high or low TOC content. See Figure S5 for the fractionation scheme

agreement with a clear shift towards drier conditions found at 4180 cal. years BP in a peatland at 200 km distance from our study area (Schellekens et al.

2014). The change from period II to III corresponds to pollen and charcoal records in the area that indicate the start of Cerrado vegetation at 7000 years BP,

Table 2 Average (Ave) C/N, $\delta^{13}\text{C}$ and $\delta^{15}\text{N}$ values of the mineral soil fractions of the three profiles (P1-H, P2-H, and P3-L); differences between profiles were significant ($P < 0.02$ for the ANOVA test).^a

Fraction	Ave. C/N			Ave. $\delta^{13}\text{C}$ (‰)			Ave. $\delta^{15}\text{N}$ (‰)		
	P3-L	P2-H	P1-H	P3-L	P2-H	P1-H	P3-L	P2-H	P1-H
Base-extractable OM	16.1 (1.9)	20.3 (2.3)	19.5 (1.0)	-19.2 (1.0)	-20.9 (0.6)	-22.5 (1.1)	8.2 (0.5)	5.4 ^b (1.0)	5.4 ^b (0.4)
Mineral-associated OM	17.3 (2.2)	21.0 (1.4)	19.9 (0.8)	-20.9 (1.0)	-21.6 ^b (0.8)	-22.0 ^b (0.4)	8.5 (1.0)	6.7 (0.5)	6.5 (0.7)
Bulk soil	18.5 (1.6)	21.3 (2.2)	21.1 (0.8)	-19.7 (0.8)	-21.4 (0.5)	-22.0 (0.4)	8.6 (0.9)	7.2 (0.8)	7.3 (0.5)

^a Standard deviation between brackets; upper 30 cm not considered; $n = 7$ for P1-H and P2-H, and $n = 5$ for P3-L

due to increasing temperature and increase of seasonality (Ledru 2002). The corresponding shifts in $\delta^{13}\text{C}$ records among the three profiles thus indicate a climatic control on $\delta^{13}\text{C}$ in these profiles, with changes in the relative contribution from trees and grasses during periods I–V. The result that shifts in TOC and $\delta^{13}\text{C}$ records occurred at the same depths (Table 1) suggests a link between the nature of the inputs and their long-term decomposability.

Spatial differences (soil properties)

In addition to temporal changes during the Holocene (Temporal differences (climatic changes) section), spatial variation in plant cover was evident by different average $\delta^{13}\text{C}$ values between profiles, with -22.0‰, -21.4‰, and -19.7‰ in profiles P1-H, P2-H, and P3-L, respectively (Table 2; Fig. 3). Mean $\delta^{13}\text{C}$ values within each time period were consistently larger in the same profiles (P3-L > P2-H > P1-H). The clearly higher $\delta^{13}\text{C}$ values in profile P3-L suggest a lower contribution from woody material to the OM in this profile. The abundance of charcoal in the same sequence (P1-H > P2-H > P3-L) supports this different tree cover (Table S3). The lower contribution from aromatic products to all fractions in profile P3-L (Table S4-2) reflects a lower amount of BC in this profile, further confirming a lower contribution from trees and shrubs that form charcoal during fires. These consistent differences between profiles suggest an additional control on vegetation composition by a local edaphic factor.

Site-specific ecological characteristics

$\delta^{15}\text{N}$ isotopic composition and C/N of bulk samples

$\delta^{15}\text{N}$ values of bulk samples varied between 5.2‰ and 9.8‰ (Table 2), which is within the range of

other Cerrado soils (Bustamante et al. 2004; Coletta et al. 2009; Craine et al. 2015). Open Cerrado shows generally $\delta^{15}\text{N}$ enriched values compared to the wooded Cerradão (Bustamante et al. 2004). Plant $\delta^{15}\text{N}$ values are often characteristic for an ecosystem, with higher values reflecting lower water availability (Handley et al. 1999). Thus, higher values of $\delta^{15}\text{N}$ in bulk samples of profile P3-L (Table 2) are consistent with lower soil water availability at this site.

The lower mean values for C/N in profile P3-L indicate an overall larger relative contribution from microbial material to this profile (Table 2). Therefore, an additional explanation for the higher values of $\delta^{13}\text{C}$ and $\delta^{15}\text{N}$ in profile P3-L could be a relatively larger contribution from microbial necromass causing an enrichment of the heavier isotopes (Craine et al. 2015; Dijkstra et al. 2006; Kramer et al. 2017). Although, the enrichment with depth in the upper 30 cm probably indeed reflects a relative increase of microbial necromass with depth (Fig. 2), this cannot explain the abrupt shifts in $\delta^{13}\text{C}$ deeper in the profile.

Composition of SOM fractions ($\delta^{13}\text{C}$ and $\delta^{15}\text{N}$ isotopic composition, C/N, and pyrolysis-GC/MS)

Comparing C/N, $\delta^{13}\text{C}$ and $\delta^{15}\text{N}$ between the SOM fractions showed that values in base-extractable OM and mineral-associated OM were similar to those in bulk samples (Fig. 5), reflecting a low contribution from the POM fractions to SOM. The C/N ratio varied from 21 to 79 in the POM fractions and from 12 to 24 in the mineral soil fractions, in agreement with similar fractions from Cerrado Ferralsols (Dick et al. 2005; Marín-Spiotta et al. 2008; Roscoe and Buurman 2003). Similar values for $\delta^{13}\text{C}$ and $\delta^{15}\text{N}$ in base-extractable OM, mineral-associated OM and bulk samples are in agreement with other studies from tropical soils (Balieiro et al. 2012; Spaccini et al. 2006). The lower $\delta^{13}\text{C}$ and $\delta^{15}\text{N}$

values in the POM fractions compared to bulk samples agree with other studies that determined the isotopic composition of POM fractions in (Cerrado) Ferralsols (Dümig et al. 2008; Kramer et al. 2017; Roscoe et al. 2001), and is attributed to abundant microbial necromass in SOM compared to plant tissues. A substantial contribution from microbial material to the mineral soil fractions of SOM is also indicated by the generally large contribution from N-containing compounds and carbohydrates in both the base-extractable OM and mineral-associated OM (Table S4-2), and by the negative correlation observed between C/N and $\delta^{15}\text{N}$ among all fractions ($r^2=0.64$, Fig. S8; Craine et al. 2015).

The similar depth trends of $\delta^{13}\text{C}$ observed in bulk samples and POM fractions ($0.28 < r^2 < 0.76$; Fig. 5) was also found by Dümig et al. (2008). This may be explained by the canopy effect that is reported to be important for Cerrado (Coletta et al. 2009) and considering that during wetter conditions there are more trees providing a larger contribution from leaves with more depleted $\delta^{13}\text{C}$ values. Contrarily to $\delta^{13}\text{C}$, $\delta^{15}\text{N}$ depth records of the POM fractions did not show a similar trend to that of the bulk, and in profiles P1-H and P3-L $\delta^{15}\text{N}$ in the free POM even showed an opposing depth trend (Fig. 5). In particular in profile P3-L the $\delta^{15}\text{N}$ depth record of the free POM clearly differed, both from other fractions in the same profile and from the same fraction in other profiles, which may point towards site-specific differences in the contribution from woody vegetation. This hypothesis of site-specific differences in vegetation composition can be examined using the pyrolysis data of the free POM that best reflects intact material. Correlations between $\delta^{15}\text{N}$ and pyrolysis products in the free POM fraction that were opposed between profiles (i.e., a positive correlation in one profile and a negative correlation in another profile) were found within the group of N-containing pyrolysis products (Supplementary material S4-4). This different behaviour of N-containing products and their relation to $\delta^{15}\text{N}$ suggests a different microbial community in profile P3-L.

Edaphic factors that may cause ecological and/or chemical spatial differences

Plant water availability

The clearly lower clay content in profile P3-L (Fig. 4b) may explain the lower contribution from

trees to this soil. Comparison of the texture in soils of Cerradão (higher tree cover) and Cerrado sensu stricto indeed showed a significantly higher clay percentage in Cerradão soils (Marimon Junior and Haridasan 2005). Clay content influences subsoil water availability in the water-limited Cerrado biome (Assis et al. 2011; Leite et al. 2018; Souza et al. 2017; Zinn et al. 2007), and deep soil layers contribute >80% of the total water used by vegetation in Cerrado (Oliveira et al. 2005). However, both P-H profiles had similar high clay content but clearly different TOC content (Fig. 4a, b). This is statistically supported by principal component analysis applied to properties of the bulk samples (Supplementary material S6). Almost all variation of TOC was explained by PC1 with loadings of -0.92, while the clay content had significant contributions from the first three components (loadings of -0.65, -0.40 and -0.51 for PC1, PC2 and PC3, respectively, Table S6). This finding is supported by a recent study on texture and TOC content of over 200 Ferralsol soil profiles, which suggested that protection by minerals is not the controlling factor on SOM stability in these soils (Martinez et al. 2021).

Because of the limited amount of water available in the topsoil during the dry season, arboreal species develop extensive root systems that reach an average of 15 m depth. Therefore, within a water-limited environment like Cerrado, physical characteristics in the subsoil may also influence water availability for roots (Jiang et al. 2020) and thereby considerably influence tree abundance in Cerrado (Leite et al. 2018). The subvertical oriented large quartz veins found at a depth of about 4 to 6 m near profile P3-L (Table S10) may favour deep drainage (Vepraskas 2005) and consequently cause lower water availability for deep roots. Furthermore, the different texture between profiles (Fig. 4b; Table S3) is likely due to local variation in saprolite type; the larger contribution of sand in P3-L is then explained by a coarser saprolite, and more clayey saprolite provides longer water storage at the saprolite-solum contact during the dry season (Jiang et al. 2020; Van der Hooven et al. 2003).

The isotopic and pyrolysis results indicate that site-specific tree-grass dynamics persisted over the past 10,000 years during which considerable temporal changes in environmental conditions occurred. It is thus very likely that the presence, depth and character of physical barriers (for water and/or roots) in the sub-surface locally controlled tree cover. The amplitude

in $\delta^{13}\text{C}$ values of the shift from periods III and IV—periods that were present in all profiles—was largest in the profile sequence P1-H < P2-H < P3-L (Table 2, Fig. 2). This is the same profile sequence as that of a decreasing contribution from trees, which supports a relation between vegetation composition and water availability, considering that the soil with the largest contribution from trees is less sensitive to drought. Also, the larger differences in $\delta^{13}\text{C}$ values between profiles in period IV compared to other periods supports this interpretation, i.e., in the driest period (period IV) the effect of limiting water availability is strongest.

Bioturbation

The relation between depth and age of charcoal fragments is different in the three profiles, with older ages at the same depth in the sequence P3-L > P2-H > P1-H (Figs. 2 and 3); this is the same profile sequence as that of the decrease in average $\delta^{13}\text{C}$ values, suggesting a faster and/or deeper downward movement of charcoal in profiles with a larger contribution from trees to the plant cover, and thus stronger bioturbation (i.e., upward transport of soil particles, see "Differences in vegetation composition ($\delta^{13}\text{C}$ of bulk samples, and charcoal)" section) in profiles with a deep humic horizon. Although the extremely intense bioturbation observed at all depths in all profiles (Fig. S9) evidences the importance of macrofauna in these soils, micromorphology provides a cumulative snapshot and cannot confirm dynamics. Considering that bioturbation is mainly carried out by termites in Cerrado (Araujo 1958; Oliveira et al. 2013), and the preference of termites for fine-textured material for construction of their nests in search of moist soils (Lamoureux and O'Kane, 2012), their activity may underlie this hypothesised local difference in bioturbation dynamics, i.e., the more compressed P3-L profile had a lower clay content (Fig. 4b), lower termite activity, and thus less bioturbation.

Decomposition

The lower C/N and higher isotope ratios in the mineral soil fractions of profile P3-L (Table 2) indicate a larger contribution from microbial material to this profile (" $\delta^{15}\text{N}$ isotopic composition and C/N of bulk samples" section). It is generally accepted to link C/N

to the degradation state of SOM. However, microbial material is not necessarily derived from decomposers. To test whether the higher amount of microbial material in profile P3-L is related to decomposers, the degradation state of plant-derived SOM was examined in pyrolysates of the mineral-associated OM fraction. Lignin pyrolysis products with a C_3 alkyl side-chain are indicative for unaltered lignin (van der Hage et al. 1993). The consistently higher values of the ratio of C_3 -guaiacol to the summed guaiacyl pyrolysis products in profile P3-L suggests a generally lower degree of decomposition in this profile (Fig. 4d). Degradation of BC as a function of depth was studied for these profiles by Justi et al. (2017), and resulted in two degradation indices composed of ratios of polyaromatic pyrolysis products, indicative for i) the degree of depolymerisation of BC and ii) the relative accumulation of condensed structures of BC (see for an explanation Supplementary material S4-3). Here, these indices are compared between profiles for the mineral-associated OM fraction (Fig. S4ab). In agreement with the lignin degradation, the degree of decomposition of BC was consistently lower in profile P3-L compared to both P-H profiles.

The combination of relatively higher microbial necromass (indicated by C/N; Table 2) but less decomposed SOM in P3-L than in P1-H and P2-H seems paradoxical, and challenges the assumption that a relatively larger contribution from microbial necromass exclusively relates to higher decomposition rates. Possible explanations include differences in the ratio of fungi to bacteria, and differential contribution by symbiotic microbes such as rhizobia and arbuscular mycorrhizal fungi in different soils. Plants that form symbioses with rhizobia and arbuscular mycorrhizal fungi are widespread in the Cerrado, and their composition is influenced by vegetation type and environmental conditions within the Cerrado biome (Marinho et al. 2019). More mycorrhizal fungi and/or rhizobia in profile P3-L would be consistent with the deviating $\delta^{15}\text{N}$ record in the free POM fraction in this profile (Fig. 5) because plants with mycorrhizal fungi are more $\delta^{15}\text{N}$ -depleted than plants without such symbiosis (2‰ on average for arbuscular mycorrhizal fungi; Craine et al. 2015). Similarly, N_2 -fixing plants have lower $\delta^{15}\text{N}$ signatures than non-fixers. A larger contribution from mycorrhizal fungi in profile P3-L is in agreement with drier conditions at this site

Table 3 A) Synthesis of the available data that relate to different soil properties between profiles (P1-H and P2-H vs. P3-L profiles), and B) their interpretation within the boundary conditions of the Cerrado, i.e., a water-limited ecosystem with abundant wildfires. Note that the qualifications higher/lower and older/younger refer to the interpretation and not to the analysed variables

	Profile P3-L	Profiles P1-H and P2-H
A. Synthesis of results		
Results	Lower	Higher
1. Trees - $\delta^{13}\text{C}$	Lower	Higher
2. Black carbon (BC) - Relative contribution from aromatic products - Microscopic charcoal (thin sections) - Macroscopic charcoal > 2 mm	Higher	Lower
3. Microbial necromass - C/N - $\delta^{13}\text{C}$, $\delta^{15}\text{N}$	Lower	Higher
4. SOM degradation state - Lignin composition - PAH composition	Negative	Positive
5. Correlation of N-compounds with $\delta^{15}\text{N}$ in the free POM - N7, N8, N10, N13, N16, N19 - N3, N14	Positive	Negative
6. Contribution from carbohydrates in the mineral-associated OM	Higher	Lower
7. Mean residence time of SOM - ^{14}C humin (given depth)	Lower	Higher
8. Age charcoal - ^{14}C charcoal (given depth)	Older	Younger
9. SOM - TOC content	Lower	Higher
10. Soil humidity - $\delta^{15}\text{N}$ - Clay content - Quartz vein in the subsoil	Lower	Higher
B. Synthesis of interpretations and directions for further research (numbers #1 to #10 refer to the results of Table 3a)		
Input material	A denser tree cover (#1) that produces more charcoal during wildfires (#2)	
Decay state of SOM	The higher contribution from microbial necromass to SOM (#3) in combination with a lower decay state of plant- and charcoal-derived SOM (#4) in profile P3-L is explained by a different microbial community, having more symbiotic mycorrhiza relative to decomposers	

Table 3 (continued)

Microbial community composition	Support for different microbial community is given by opposing correlations between profiles of N-containing products with $\delta^{15}\text{N}$ in the light fraction (#5), a significantly higher carbohydrate contribution in the mineral-associated OM of profile P3-L (#6), and a lower mean residence time (#7) in combination with a lower SOM degradation state (#4) in this profile
Bioturbation	A lower ^{14}C of charcoal fragments (at similar depth; #8) suggests less bioturbation in profile P3-L, which results in less active upward transport of fine soil particles per unit of time, and consequently a slower (inactive) residual downward movement of coarser materials (too large to pass through the termites or other soil fauna) that includes macroscopic surface litter such as charcoal
Soil humidity	These results provide cumulative evidence that the higher TOC content in both profiles with a thick humic A-horizon (#9) is explained by higher soil humidity. Apart from the observed factors that determine soil humidity (#10), it is well-known that soil humidity governs tree-grass vegetation patterns (input material), soil faunal activity (bioturbation), and microbial community structure (mycorrhiza) in the Cerrado

as indicated by $\delta^{13}\text{C}$, because plants with mycorrhizal symbioses are more drought tolerant (Frosi et al. 2016). The plant, in turn, provides the fungi with carbohydrates, that were significantly higher in the mineral-associated OM fraction of profile P3-L (43.2% carbohydrates) compared to both P-H profiles (< 35%; Table S4-2).

Implications for future research

An overview of the results that relate to input and decay of SOM are given in Table 3a, and their combined interpretation (Table 3b) provides directions for further research.

Environmental reconstruction

Our data indicate that Cerrado soils contain information on Holocene environmental conditions. Comparison of the $\delta^{13}\text{C}$ records sampled at relatively high- and low-resolution (10 cm intervals vs. pedogenic horizons) demonstrates the importance of high-resolution sampling to identify temporal changes in vegetation composition (Calegari et al. 2013; Chiapini et al. 2018): i.e., the abrupt shifts are exclusively evidenced in the high-resolution records (Fig. 3; Table 1). This sampling at 10 cm intervals allowed reconstructing changes in vegetation composition with differences in $\delta^{13}\text{C}$ as low as 0.3‰, greatly extending the generally accepted limit of 4‰ for this purpose (Desjardins et al. 1996). This is in particular valid with an increase of trees because depletion of $\delta^{13}\text{C}$ can exclusively be linked to a vegetation change, while enrichment may be additionally influenced by other factors such as microbial reworking.

Methodological recommendations for environmental reconstruction from Cerrado soils include high-resolution sampled $\delta^{13}\text{C}$ records (10 cm intervals) to visualise shifts in $\delta^{13}\text{C}$, a minimum profile depth of 2 m, and ^{14}C dating of both humin and charcoal. Ferralsols with low TOC content (i.e., without deep Umbric horizon) best reflected environmental changes because of their compressed age (i.e., older charcoal for similar depths), and their lower water availability and corresponding larger sensibility for water stress in trees (larger ranges in $\delta^{13}\text{C}$), reflecting

that growth of woody vegetation in these water-limited ecosystems is near threshold values.

Carbon sequestration

The consistently higher TOC content in the sequence P1-H > P2-H > P3-L, indicates that the differences in TOC content between the soil profiles have persisted over thousands of years. The fact that soils with a deep humic horizon in the study area were persistently present next to Ferralsols without such horizon, notwithstanding the climatic variation during the Holocene, clearly indicates that site characteristics must underlie their formation, in agreement with a dominant control of local differences in edaphic factors on soil carbon storage found for Bolivian (Maezumi et al. 2015) and Guyanese (Black et al. 2021) savannah. The consistent spatial differences in long-term $\delta^{13}\text{C}$ records at a local scale suggest that soil carbon storage in Cerrado is controlled by water availability, and may indicate relatively large sensitivity of soil carbon storage to minor changes in climatic conditions in Cerrado ecosystems. Knowledge of such edaphic threshold behaviour for the carbon cycle is extremely important because a small change in environmental forcing, e.g., global warming, will result in a large response (Scheffer et al. 2001).

Conclusions

Long-term carbon storage in Brazilian Cerrado soils was caused by site-specific differences in tree-grass composition and bioturbation. Soils with an OM-rich thick A-horizon had more trees, more charcoal, and a higher activity of soil macrofauna. Both spatial and temporal differences in the contribution from arboreal vegetation were controlled by water availability, with relatively wet conditions causing an increase of trees and thereby an increase of charcoal during fires. This larger contribution of charcoal together with its relative persistence to degradation and faster downward movement by bioturbation caused the larger TOC content in the profiles with profundihumic properties. For the Cerrado soils of the study area, climate determined the boundary conditions (i.e., water deficiency and fire-dependent ecosystems) for the formation of the

deep A-horizon, within which edaphic factors locally controlled tree-grass dynamics by water availability.

Acknowledgements This research was supported by the São Paulo Research Foundation (FAPESP) projects 2014/23969-0, 2014/21128-8 and 2013/03953-9, and the Flanders Research Foundation (FWO; grant number: 12ZY320N/SW). The last author is supported by National Council for Scientific and Technological Development – CNPq, grant 301818/2017-7. We thank two anonymous reviewers for their critical and valuable comments.

Data Availability Data will be made available on request.

Declarations

Competing interests The authors have no relevant financial or non-financial interests to disclose.

References

- Angst G, Mueller KE, Nierop KGI, Simpson MJ (2021) Plant- or microbial-derived? A review on the molecular composition of stabilized soil organic matter. *Soil Biol Biochem* 156:108189. <https://doi.org/10.1016/j.soilbio.2021.108189>
- Araujo RL (1958) Contribuição à biogeografia dos térmitas de Minas Gerais, Brasil. *Arq Instituto Biol* 25:219–236
- Assis ACC, Coelho RM, Pinheiro ES, Durigan G (2011) Water availability determines physiognomic gradient in an area of low-fertility soils under Cerrado vegetation. *Plant Ecol* 212:1135–1147. <https://doi.org/10.1007/s11258-010-9893-8>
- Balheiro FC, Benites VM, Caiafa AN, Alves BJR, Fontana A, Canellas LP (2012) Vegetation influence on organic matter source of black soils from high altitude rocky complexes traced by ^{13}C and ^{15}N isotopic techniques. *CATENA* 99:97–101. <https://doi.org/10.1016/j.catena.2012.06.004>
- Black JE, Wagner T, Abbott GD (2021) Assessing lignin decomposition and soil organic carbon contents across a tropical savannah-rainforest boundary in Guyana. *Front for Glob Change* 4:629600. <https://doi.org/10.3389/ffgc.2021.629600>
- Boutton TW, Archer SR, Midwood AJ, Zitzer SF, Bol R (1998) $\delta^{13}\text{C}$ values of soil organic carbon and their use in documenting vegetation change in a subtropical savanna ecosystem. *Geoderma* 82:5–41
- Bueno ML, Dexter KG, Pennington RT, Pontara V, Mesquite Neves D, Ratter JA, de Oliveieira-Filho AT (2018) The environmental triangle of the Cerrado domain: ecological factors driving shifts in tree species composition between forests and savannas. *J Ecol* 106:2109–2120. <https://doi.org/10.1111/1365-2745.12969>
- Bustamante MMC, Martinelli LA, Silva DA, Camargo PB, Klink CA, Domingues TF, Santos RV (2004) ^{15}N natural

- abundance in woody plants and soils of central Brazilian savannas (Cerrado). *Ecol Appl* 14:200–213. <https://doi.org/10.1890/01-6013>
- Calegari MR, Madella M, Vidal-Torrado P, Pessenda LCR, Marques FA (2013) Combining phytoliths and $\delta^{13}\text{C}$ matter in Holocene palaeoenvironmental studies of tropical soils: an example of an Oxisol in Brazil. *Quatern Int* 287:47–55. <https://doi.org/10.1016/j.quaint.2011.11.012>
- Chiapini M, Schellekens J, Calegari MR, de Almeida JA, Buurman P, de Camargo PB, Vidal-Torrado P (2018) Formation of black carbon rich ‘sombriç’ horizons in the subsoil – A case study from subtropical Brazil. *Geoderma* 314:232–244. <https://doi.org/10.1016/j.geoderma.2017.10.031>
- Coletta LD, Nardoto GB, Latansio-Aidar SR, da Rocha HR, Aidar MPM, Ometto JPHB (2009) Isotopic view of vegetation and carbon and nitrogen cycles in a Cerrado ecosystem, southeastern Brazil. *Sci Agr* 66:467–475. <https://doi.org/10.1590/S0103-90162009000400006>
- Craine JM, Brookshire ENJ, Cramer MD, Hasselquist NJ, Koba K, Marin-Spiotta E, Wang L (2015) Ecological interpretations of nitrogen isotope ratios of terrestrial plants and soils. *Plant Soil* 396:1–26. <https://doi.org/10.1007/s11104-015-2542-1>
- Desjardins T, Filho AC, Mariotti A, Chauvel A, Girardim C (1996) Changes of the forest-savanna boundary in Brazilian Amazonia during the Holocene as revealed by soil organic carbon isotope ratios. *Oecologia* 108:749–756. <https://doi.org/10.1007/BF00329051>
- Dick DP, Gonçalves CN, Dalmolin RSD, Knicker H, Klamt E, Kögel-Knabner I, Simões ML, Martin-Neto L (2005) Characteristics of soil organic matter of different Brazilian Ferralsols under native vegetation as a function of soil depth. *Geoderma* 124:319–333. <https://doi.org/10.1016/j.geoderma.2004.05.008>
- Dijkstra P, Ishizu A, Doucett R, Hart SC, Schwartz E, Menyailo OV, Hungate BA (2006) ^{13}C and ^{15}N natural abundance of the soil microbial biomass. *Soil Biol Biochem* 38:3257–3266. <https://doi.org/10.1016/j.soilbio.2006.04.005>
- Dümmig A, Schad P, Rumpel C, Dignac MF, Kögel-Knabner I (2008) Araucaria forest expansion on grassland in the southern Brazilian highlands as revealed by ^{14}C and $\delta^{13}\text{C}$ studies. *Geoderma* 145:143–157. <https://doi.org/10.1016/j.geoderma.2007.06.005>
- Eiten G (1972) The cerrado vegetation of Brazil. *Bot Rev* 38:139–148. <https://doi.org/10.1007/BF02859158>
- Frosi G, Barros VA, Oliveira MT, Santos M, Ramos DG, Maia LC, Santos MG (2016) Symbiosis with AMF and leaf Pi supply increases water deficit tolerance of woody species from seasonal dry tropical forest. *J Plant Physiol* 207:84–93. <https://doi.org/10.1016/j.jplph.2016.11.002>
- Handley LL, Austin AT, Robinson D, Scrimgeour CM, Raven JA, Heaton HE, Schmidt S, Stewart GR (1999) The ^{15}N natural abundance ($\delta^{15}\text{N}$) of ecosystem samples reflects measures of water availability. *Aust J Plant Physiol* 26:185–199. <https://doi.org/10.1071/PP98146>
- IBGE - Instituto Brasileiro de Geografia e Estatística (2012) Manual Técnico da Vegetação Brasileira. Série Manuais Técnicos em Geociências 1, (2nd ed). IBGE, Rio de Janeiro.
- IUSS Working Group WRB - World reference base for soil resources, update 2015. International soil classification system for naming soils and creating legends for soils maps. (Resources Reports No. 106). Rome: Food and Agriculture Organization of the United Nations
- Jantalia CP, Resck DVS, Alves BJR, Zotarelli L, Urquiaga S, Boddey RM (2007) Tillage effect on C stocks of a clayey Oxisol under a soybean-based crop rotation in the Brazilian Cerrado region. *Soil till Res* 95:97–109. <https://doi.org/10.1016/j.still.2006.11.005>
- Jiang Z, Liu H, Wang H, Peng J, Meersmans J, Gree SM, Quine TA, Wu X, Song Z (2020) Bedrock geochemistry influences vegetation growth by regulating the regolith water holding capacity. *Nat Commun* 11:2392. <https://doi.org/10.1038/s41467-020-16156-1>
- Justi M, Schellekens J, Camargo PB, Vidal-Torrado P (2017) Long-term degradation effects on the molecular composition of black carbon in Brazilian Cerrado soils. *Org Geochem* 113:196–209. <https://doi.org/10.1016/j.orggeochem.2017.06.002>
- Klamt E, Van Reeuwijk LP (2000) Evaluation of morphological, physical and chemical characteristics of Ferralsols and related soils. *Rev Bras Cienc Solo* 24:573–687. <https://doi.org/10.1590/S0100-06832000000300011>
- Kramer MG, Lajtha K, Aufdenkampe AK (2017) Depth trends of soil organic matter C: N and ^{15}N natural abundance controlled by association with minerals. *Biogeochemistry* 136:237–248. <https://doi.org/10.1007/s10533-017-0378-x>
- Lamoureux S, O’Kane MA (2012) Effects of termites on soil cover system performance. Proceedings of the Seventh International Conference on Mine Closure, Australia, 433–446. https://doi.org/10.36487/ACG_rep/1208_38_Lamoureux
- Ledru MP (2002) Late Quaternary history and evolution of the Cerrados as revealed by palynological records. In: Oliveira PS, Marquis RJ (eds) The Cerrados of Brazil. Ecology and Natural History of a neotropical savannah, Columbia University Press, New York, pp 33–50
- Leite MB, Xavier RO, Sanches Oliveira PT, Gomes Silva FK, Silva Matos DM (2018) Groundwater depth as a constraint on the woody cover in a neotropical savanna. *Plant Soil* 426:1–15. <https://doi.org/10.1007/s11104-018-3599-4>
- Luo Z, Viscarra-Rossel RA, Qian T (2021) Similar importance of edaphic and climatic factors for controlling soil organic carbon stocks of the world. *Biogeosciences* 18:2063–2073. <https://doi.org/10.5194/bg-18-2063-2021>
- Maezumi SY, Power MJ, Mayle FE, McLauchlan KK, Iriarte J (2015) Effects of past climate variability on fire and vegetation in the cerrado savanna of the Huanchaca Mesetta, NE Bolivia. *Clim past* 11:835–853. <https://doi.org/10.5194/cp-11-835-2015>
- Marimon Junior BH, Haridasan M (2005) Comparação da vegetação arbórea e características edáficas de um cerrado e um cerrado sensu stricto em áreas adjacentes sobre solo distrófico no leste de Mato Grosso, Brasil. *Acta Bot Bras* 19:913–926. <https://doi.org/10.1590/S0102-33062005000400026>
- Marinho F, Oehl F, da Silva IR, Coyne D, Veras JSN, Maia LC (2019) High diversity of arbuscular mycorrhizal fungi in natural and anthropized sites of a Brazilian tropical dry

- forest (Caatinga). *Fungal Ecol* 40:82–91. <https://doi.org/10.1016/j.funeco.2018.11.014>
- Marín-Spiotta E, Swanston CW, Torn MS, Silver WL, Burton SD (2008) Chemical and mineral control of soil carbon turnover in abandoned tropical pastures. *Geoderma* 143:49–62. <https://doi.org/10.1016/j.geoderma.2007.10.001>
- Marques FA, Buurman P, Schellekens J, Vidal-Torrado P (2015) Molecular chemistry in humic Ferralsols from Brazilian Cerrado and forest biomes indicates a major contribution from black carbon in the subsoil. *J Anal Appl Pyrol* 113:518–528. <https://doi.org/10.1016/j.jaap.2015.03.016>
- Martinez P, Silva LCR, Calegari MR, Barbosa de Camargo P, Vidal-Torrado P, Kleber M (2021) Carbon stocks in umbricferralsols driven by plant productivity and geomorphic processes, not by mineral protection. *Earth Surf Proc Land* 1–18. <https://doi.org/10.1002/esp.5262>
- Nepstad DC, Klink CA, Uhl C, Vieira IC, Lefebvre P, Pedlowski M, Matricardi E, Negreiros G, Brown IF, Amaral E, Homma A, Walker R (1997) Land use in Amazonia and Cerrado of Brazil. *Cienc Cult* 49:73–83
- Oliveira RS, Bezerra L, Davidson EA, Pinto F, Klink CA, Nepstad DC, Moreira A (2005) Deep root function in soil water dynamics in Cerrado savannas of central Brazil. *Funct Ecol* 19:574–581. <https://doi.org/10.1111/j.1365-2435.2005.01003.x>
- Oliveira DE, Carrizo TF, Brandão D (2013) Species composition of termites (Isoptera) in different Cerrado vegetation physiognomies. *Sociobiology* 60:190–197. <https://doi.org/10.13102/sociobiology.v60i2.190-197>
- Oliveras I, Malhi Y (2016) Many shades of green: the dynamic tropical forest-savannah transition zones. *Phil Trans R Soc B* 371:20150308. <https://doi.org/10.1098/rstb.2015.0308>
- Pessenda LCR (1996) The use of carbon isotopes (^{13}C , ^{14}C) in soil to evaluate vegetation changes during the Holocene in Central Brazil. *Radiocarbon* 38:191–201. <https://doi.org/10.1017/S0033822200017562>
- Pessenda LCR, Gomes BM, Aravena R, Ribeiro AS, Boulet R, Gouveia SEM (1998) The carbon isotope record in soils along a forest–Cerrado ecosystem transect: implications for vegetation changes in the Rondonia state, southwestern Brazilian Amazon region. *Holocene* 8:631–635. <https://doi.org/10.1191/095968398673187182>
- Pessenda LCR, Gouveia SEM, Aravena R, Boulet R, Valencia EPE (2004) Holocene fire and vegetation changes in southeastern Brazil as deduced from fossil charcoal and soil carbon isotopes. *Quatern Int* 114:35–43. [https://doi.org/10.1016/S1040-6182\(03\)00040-5](https://doi.org/10.1016/S1040-6182(03)00040-5)
- Prietzl J, Hiesch S, Harrington G, Müller S (2020) Microstructural and biochemical diversity of forest soil organic surface layers revealed by density fractionation. *Geoderma* 366:114262. <https://doi.org/10.1016/j.geoderma.2020.114262>
- Reimer PJ, Bard E, Bayliss A, Beck JW, Blackwell PG, Bronk Ramsey C, Buck CE, Cheng H, Edwards RL, Friedrich M, Grootes PM, Guilderson TP, Haflidason H, Hajdas I, Hatté C, Heaton TJ, Hogg AG, Hughen KA, Kaiser KF, Kromer B, Manning SW, Niu M, Reimer RW, Richards DA, Scott EM, Southon JR, Turney CSM, van der Plicht J (2013) IntCal13 and MARINE13 radiocarbon age calibration curves 0–50000 years cal BP. *Radiocarbon* 55:1869–1887. https://doi.org/10.2458/azu_js_rc.55.16947
- Roscoe R, Buurman P (2003) Tillage effects on soil organic matter in density fractions of a Cerrado Oxisol. *Soil Till Res* 70:107–119. [https://doi.org/10.1016/S0167-1987\(02\)00160-5](https://doi.org/10.1016/S0167-1987(02)00160-5)
- Roscoe R, Buurman P, Velthorst EJ, Pereira JAA (2000) Effects of fire on soil organic matter in a ‘cerrado sensu stricto’ from southeast Brazil as revealed by changes in $\delta^{13}\text{C}$. *Geoderma* 95:141–160. [https://doi.org/10.1016/S0016-7061\(99\)00089-0](https://doi.org/10.1016/S0016-7061(99)00089-0)
- Roscoe R, Buurman P, Velthorst EJ, Vasconcellos CA (2001) Soil organic matter dynamics in density and particle-size fractions as revealed by the ^{13}C isotopic ratio in a Cerrado’s Oxisol. *Geoderma* 104:185–202. [https://doi.org/10.1016/S0016-7061\(01\)00080-5](https://doi.org/10.1016/S0016-7061(01)00080-5)
- Schaefer CER (2001) Brazilian latosols and their B horizon microstructure as long-term biotic constructs. *Aust J Soil Res* 39:909–926. <https://doi.org/10.1071/SR00093>
- Scheffer M, Carpenter S, Foley JA, Folke C, Walker B (2001) Catastrophic shifts in ecosystems. *Nature* 413:591–596. <https://doi.org/10.1038/35098000>
- Schellekens J, Horák-Terra I, Buurman P, Silva AC, Vidal-Torrado P (2014) Holocene vegetation and fire dynamics in central-eastern Brazil: molecular records from the Pau de Fruta peatland. *Org Geochem* 77:32–42. <https://doi.org/10.1016/j.orggeochem.2014.08.011>
- Scurlock JMO, Hall DO (1998) The global carbon sink: a grassland perspective. *Global Change Biol* 4:229–223. <https://doi.org/10.1046/j.1365-2486.1998.00151.x>
- Silva AC, Vidal-Torrado P (1999) Gênese dos Latossolos Húmicos e sua relação com a evolução da paisagem numa área cratônica do sul de Minas Gerais. *Rev Bras Cienc Solo* 23:329–341. <https://doi.org/10.1590/S0100-06831999000200017>
- Six J, Elliott ET, Paustian K, Doran JW (1998) Aggregation and soil organic matter accumulation in cultivated and native grassland soils. *Soil Sci Soc Am J* 62:1367–1377. <https://doi.org/10.2136/sssaj1998.03615995006200050032x>
- Smith KR, Waring BG (2019) Broad-scale patterns of soil carbon (C) pools and fluxes across semiarid ecosystems are linked to climate and soil texture. *Ecosystems* 22:742–753. <https://doi.org/10.1007/s10021-018-0299-0>
- Souza IF, Almeida LFJ, Jesus GL, Kleber M, Silva IR (2017) The mechanisms of organic carbon protection and dynamics of C-saturation in Oxisols vary with particle-size distribution. *Eur J Soil Sci* 68:726–739. <https://doi.org/10.1111/ejss.12463>
- Spaccini R, Mbagwu JSC, Conte P, Piccolo A (2006) Changes of humic substances characteristics from forested to cultivated soils in Ethiopia. *Geoderma* 132:9–19. <https://doi.org/10.1016/j.geoderma.2005.04.015>
- Van der Hage ERE, Mulder MM, Boon JJ (1993) Structural characterization of lignin polymers by temperature-resolved in-source pyrolysis—mass spectrometry and Curie-point pyrolysis—gas chromatography/mass spectrometry. *J Anal Appl Pyrol* 25:149–183. [https://doi.org/10.1016/0165-2370\(93\)80038-2](https://doi.org/10.1016/0165-2370(93)80038-2)
- Van der Hooven SJ, Solomon DK, Moline GR (2003) Modeling unsaturated flow and transport in the saprolite of

- the fractured sedimentary rocks: Effects of periodic wetting and drying. *Water Resour Res* 39:1186. <https://doi.org/10.1029/2002WR001926>
- Vepraskas MJ (2005) Predicting contaminant transport along quartz veins above the water table in a mica-schist saprolite. *Geoderma* 126:47–57. <https://doi.org/10.1016/j.geoderma.2004.11.006>
- von Lützw M, Kögel-Knabner I, Ekschmitt K, Matzner E, Guggenberger G, Marschner B, Flessa H (2006) Stabilization of organic matter in temperate soils: mechanisms and their relevance under different soil conditions - a review. *Eur J Soil Sci* 57:426–445
- Wiesmeier M, Urbanski L, Hobbey E, Lang B, von Lützw M, Marín-Spiotta E, van Wesemael B, Rabot E, Ließ M, Garcia-Franco N, Wollschläger U, Vogel H-J, Kögel-Knabner I (2019) Soil organic carbon storage as a key function of soils – A review of drivers and indicators at various scales. *Geoderma* 333:149–162. <https://doi.org/10.1016/j.geoderma.2018.07.026>
- Wilkinson MT, Richards PJ, Humphreys GS (2009) Breaking ground: pedological, geological, and ecological implications of soil bioturbation. *Earth-Sci Rev* 97:257–272. <https://doi.org/10.1016/j.earscirev.2009.09.005>
- Zinn YL, Lal R, Bigham JM, Resck DVS (2007) Edaphic controls on soil organic carbon retention in the Brazilian Cerrado: texture and mineralogy. *Soil Sci Soc Am J* 71:1204–1214. <https://doi.org/10.2136/sssaj2006.0014>

Publisher's note Springer Nature remains neutral with regard to jurisdictional claims in published maps and institutional affiliations.

Springer Nature or its licensor (e.g. a society or other partner) holds exclusive rights to this article under a publishing agreement with the author(s) or other rightsholder(s); author self-archiving of the accepted manuscript version of this article is solely governed by the terms of such publishing agreement and applicable law.